Friction compensation of gantry crane model based on the B-spline neural compensator

Jadranko Matuško*, Fetah Kolonić*, Šandor Ileš *, Alojz Slutej†
*Faculty of Electrical Engineering and Computing, Zagreb, Croatia,
e-mail: *jadranko.matusko@fer.hr, fetah.kolonic@fer.hr, sandor.iles@fer.hr*
†ABB, Vasteras, Sweden, e-mail: *alojz.slutej@se.abb.com*

***Abstract*—Fast and accurate positioning and swing minimization of the containers and other loads in crane manipulation are demanding and in the same time conflicting tasks. For accurate positioning, the main problem is nonlinear friction compensation, especially in the low speed region. In this paper authors propose position controller realized as hybrid controller. It consists of the conventional linear state feedback controller with additional friction self-learning neural compensator in the feedforwad loop. Self-learning compensator is based on the B-spline artificial neural network which consists of the one hidden layer of the B-spline second order functions. The experimental results show that friction compensator is able to remove position error in steady state.**

***Index Terms*—Single Pendulum Gantry, Neural Network, Friction Compensation, B-spline network, on-line network learning.**

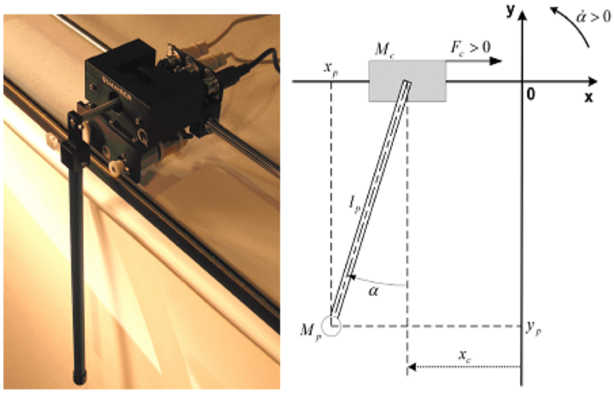

Fig. 1. Single pendulum gantry (SPG) electromechanical model as experimental model of gantry crane

I. Introduction

Translational gantry cranes are widely used for the heavy loads transfer in modern industrial systems. The problem faced in load transfer is a negative influence of the crane acceleration required for the motion. Any change of the reference position causes an undesirable load swing, having negative consequences on the system control and safety performances.

In order to achieve acceptable system performances for a fast load positioning (i.e. minimal load transfer time), the swing of the suspended load should be controlled as well. This conflicting control demands can be solved with state feedback controller, designed according to linear quadratic optimum criteria, [3]. This design technique is imposed as a logical solution and it is used by several authors for solving similar control tasks.

Although the load swing problem is generally nonlinear most of the solutions are based on the linearized mathematical model. Typical control approaches are adaptive (gain-scheduling logic with optimal controllers used by Corriga, Giua and Usai in [3]), optimal (Wang and Surgenor in [13]) or robust (G. Bartolini et al. in [1]), applied on the similar types of the electromechanical systems.

Due to crane system complexity and the fact that linearised mathematical model only partially represents the real system, some authors used fuzzy controller, [8], [6], [10]. Controller based on fuzzy logic can partially solve an undesirable effects caused by the system nonlinearities, [10]. However, neither of proposed techniques provide solution for the main problem of accurate positioning - friction. Due to its highly nonlinear characteristics complex nonlinear behavior like limit cycle may occur if the controller includes the integral action. In order to reduce or eliminate the impact of friction, a self-learning compensator is proposed as additional feedforward loop to conventional linear state feedback controller. It is based artificial neural network with one hidden layer of the B-spline second order functions.

II. Mathematical Model of the Single Pendulum Gantry

The single pendulum gantry mounted on the linear cart is presented in the Fig.1, [4]. When facing the cart, a positive direction of the cart motion is to the right and a positive sense of the pendulum rotation is defined as counter clockwise. Also, the zero angle, corresponds to a suspended pendulum vertical rest down position. Single pendulum gantry can be represented as a system with one input u (motor voltage), and two outputs: α (pendulum angle) and x_c (cart position). Mathematical equations of the system motion can be derived via Lagrange equations, by defining total potential and kinetic energy of the system as a functions of generalized coordinates: cart position x_c and pendulum swing angle α. The result is the nonlinear model represented by equations (1) and (2).

After linearisation around pendulum angle $\alpha = 0$, the linear model, given by equations (3) and (4), is obtained. The parameters of the single pendulum gantry linear

$$\ddot{x}_c = \frac{-(I_p + M_p l_p^2) B_{eq} \cdot \dot{x}_c + (M_p^2 l_p^3 + l_p M_p I_p)\sin(\alpha) \cdot \dot{\alpha}^2 + M_p l_p \cos(\alpha) B_p \cdot \dot{\alpha}}{(M_c + M_p) I_p + M_c M_p l_p^2 + M_p^2 l_p^2 \sin^2(\alpha(t))} + \\ + \frac{M_p^2 l_p^2 g \cos(\alpha)\sin(\alpha) - (I_p + M_p l_p^2)(\frac{\eta_g K_g^2 \eta_m K_t K_m \cdot \dot{x}_c}{R_m r_{mp}^2} + (I_p + M_p l_p^2)\frac{\eta_g K_g \eta_m K_t}{R_m r_{mp}} U_m)}{(M_c + M_p) I_p + M_c M_p l_p^2 + M_p^2 l_p^2 \sin^2(\alpha)} \tag{1}$$

$$\ddot{\alpha} = \frac{-(M_c + M_p) B_p \cdot \dot{\alpha} - M_p^2 l_p^2 \sin(\alpha)\cos(\alpha) \cdot \dot{\alpha}^2 + M_p l_p \cos(\alpha) B_{eq} \cdot \dot{x}_c}{(M_c + M_p) I_p + M_c M_p l_p^2 + M_p^2 l_p^2 \cdot \sin^2(\alpha)} + \\ + \frac{-(M_c + M_p) M_p g l_p \sin(\alpha) + M_p l_p \cos(\alpha)\frac{\eta_g K_g^2 \eta_m K_t K_m \cdot \dot{x}_c}{R_m r_{mp}^2} - M_p l_p \cos(\alpha)\frac{\eta_g K_g \eta_m K_t}{R_m r_{mp}} U_m)}{(M_c + M_p) I_p + M_c M_p l_p^2 + M_p^2 l_p^2 \cdot \sin^2(\alpha)} \tag{2}$$

$$\begin{bmatrix} \dot{x}_c(t) \\ \dot{\alpha}(t) \\ \ddot{x}_c(t) \\ \ddot{\alpha}(t) \end{bmatrix} = \begin{bmatrix} 0 & 0 & 1 & 0 \\ 0 & 0 & 0 & 1 \\ 0 & 1.5216 & -11.6513 & 0.0049 \\ 0 & -26.1093 & 26.8458 & -0.0841 \end{bmatrix} \cdot \begin{bmatrix} x_c(t) \\ \alpha(t) \\ \dot{x}_c(t) \\ \dot{\alpha}(t) \end{bmatrix} + \begin{bmatrix} 0 \\ 0 \\ 1.5304 \\ -3.5261 \end{bmatrix} \cdot U_m(t) \tag{3}$$

$$\begin{bmatrix} x_c(t) \\ \alpha(t) \end{bmatrix} = \begin{bmatrix} 1 & 0 & 0 & 0 \\ 0 & 1 & 0 & 0 \end{bmatrix} \cdot \begin{bmatrix} x_c(t) \\ \alpha(t) \\ \dot{x}_c(t) \\ \dot{\alpha}(t) \end{bmatrix} \tag{4}$$

model are given in Table I.

TABLE I
PARAMETERS OF THE SINGLE PENDULUM GANTRY SYSTEM

Parameters	Description
$B_{eq} = 5.4[Nms/rad]$	Equivalent viscous damping coefficient as seen at the motor pinion
$B_p = 0.0024[Nm/s]$	viscous damping coefficient as seen at the pendulum axis
$\eta_g = 1$	Planetary gearbox efficiency
$\eta_m = 1$	Motor efficiency
$g = 9.81[m/s^2]$	Gravitational constant of earth
$J_p = 0.0078838[kgm^2]$	Pendulum moment of inertia
$J_m = 3.9e-7[kgm^2]$	Rotor moment of inertia
$K_g = 3.71$	Planetary gearbox gear ratio
$K_m = 0.0076776$	Back electro-motive force (EMF) constant
$K_t = 0.007683$	Motor torque constant
$l_p = 0.3302[m]$	Pendulum length from pivot to center of gravity
$M_c = 1.0731[kg]$	Lumped mass of the cart system, including the rotor inertia
$M_p = 0.23[kg]$	Pendulum mass
$R_m = 2.6[\Omega]$	Motor armature resistance
$r_{mp} = 0.00635[m]$	Motor pinion radius

A. Friction effect

Above presented mathematical model of the Single Pendulum Gantry does not include friction model. However, friction is almost unavoidable effect in mechanical systems and it may seriously degrade the performance of the control system. This problem is specially significant when high precision positioning is required. Friction

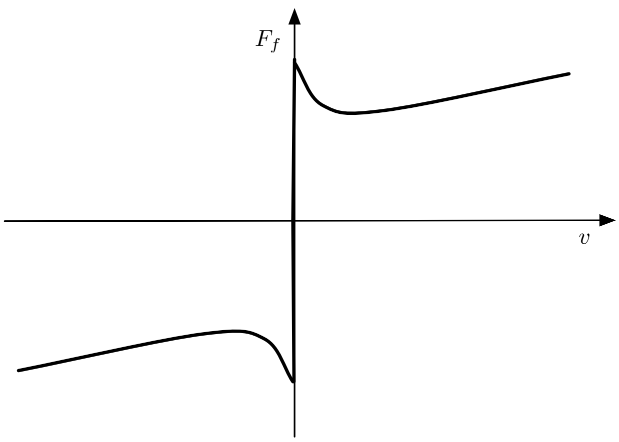

Fig. 2. Typical friction characteristic

characteristic is generally highly nonlinear and may also vary with time. In addition, identification of the friction characteristic is complex task. Typical friction characteristic is shown in Fig. 2. It can be seen that friction force reaches its peak value at very low speeds ($v \approx 0$) and this portion of the friction characteristics is usually regarded to as a static friction. Such the increase in friction force when velocity approaches zero is the main cause of the steady state error in positioning systems. It is important to note that augmentation of the controller with an integral action cannot eliminate such the error. Moreover, it may result in complex nonlinear effect known as stick-slip motion which can significantly reduce the life cycle of the system components (e.g. actuators, gears). Therefore, feedforward compensation based on B-spline neural network will be used in this paper.

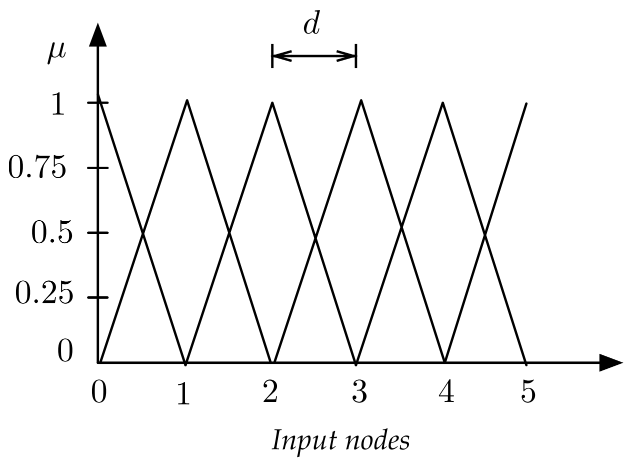

Fig. 3. B-spline second order functions

III. B-SPLINE NEURAL NETWORKS

A. Network Structure

B-spline neural network (BSN) is a special type of neural networks that use B-spline functions as basis functions, [2]. One dimensional n-order B-spline network consists of set of $(n-1)$-order polynomial functions and hence unknown function is approximated by piecewise polynomial functions of $(n-1)$-order. The higher order of B-spline functions used the better and smoother approximation is obtained with increased network complexity. It has been proven that B-spline second order functions (Fig.3) usually gives good results with simple and fast parameters adaptation. Since the numerical simplicity is an important criteria for compensator design, B-spline functions represent an acceptable and reasonable choice.

Axis x, in Fig.3, represents neural network input nodes, while axis y represents the nodes membership to the polynomial functions, $\mu \in [0,1]$. The limits of the particular polynomial functions are determined by the node vector:

$$\lambda = \left[\begin{array}{ccc} \lambda_0 & \lambda_1 & ...\lambda_{N_k} \end{array}\right] \in \Re^{N_{k-1}}. \tag{1}$$

The membership to i-th B-spline function (i-th polynomial function) of n-order is calculated according to:

$$\begin{aligned} \mu_i^n(x) = & \left(\frac{x-\lambda_{i-n}}{\lambda_{i-1}-\lambda_{i-n}}\right)\mu_{i-1}^{n-1}(x) + \\ & + \left(\frac{\lambda_i - x}{\lambda_i - \lambda_{i-n+1}}\right)\mu_i^{n-1}(x). \end{aligned} \tag{2}$$

For each input signal, the shape and distribution of B-spline functions are arranged in the way that the sum of all membership functions equals to one:

$$\forall x \in R, \sum_{i=1}^{N_k} \mu_i(x) = 1. \tag{3}$$

The output of the B-spline network is the weighted sum of the outputs of B-spline neurons, given by the following equation:

$$y = \sum_{i=1}^{N_k} \mu_i(x) \cdot w_i. \tag{4}$$

If smoother transient between networks nodes is necessary, then higher order B-spline functions should be used. However, the drawback is complex computation and more computer resources needed for algorithm implementation.

B. B-Spline Network Learning

The learning of the BSN network parameters can be performed either off-line, based on previously collected set of I/O data, or on-line, during the normal operating condition. Since the aim of the paper is compensation of an unknown and unpredictable system's nonlinearities, the network parameters need to be adapted on-line. Usually only BSN weighting coefficients w_i are adapted while the shape and distribution are set off-line based on a-priory knowledge about the system to be approximated. Such the approach not only simplifies the learning process but also allow relatively simple stability analysis.

Generally the adaptation of the BSN weighting coefficients is performed by minimizing the appropriate cost function. Selected cost function to be minimized during the learning process, is given by:

$$J = \frac{1}{2}\left(y_d - y\right)^2. \tag{5}$$

Using the rule

$$\Delta w_i = -\gamma \frac{\partial J}{\partial w_i} = \gamma \left(y_d - y\right) \frac{\partial y}{\partial w_i} \tag{6}$$

and inserting (4) in (6) yields

$$\Delta w_i = \gamma \left(y_d - y\right) \frac{\partial \sum_{j=1}^{N_k} \mu_j(x) \cdot w_j}{\partial w_i} = \gamma \left(y_d - y\right) \mu_i(x), \tag{7}$$

where Δw_i is adaptation of weighting coefficient for i-th B-spline function and γ is learning rate.

Instead of using the output error $e(t) = r(t) - y(t)$ as a measure of control performance it is also possible to use the output of the feedback controller as performance measure. Indeed, when a perfect tracking is achieved (i.e. $r(t) = y(t)$) the output of the feedback controller u_c is equal to zero while existence of the tracking error will result in nonzero control signal. Therefore, the adaptation law for the BSN network parameters, used in this paper, is given by:

$$\Delta w_i = \gamma u_c \frac{\partial \sum_{j=1}^{N_k} \mu_j(x) \cdot w_j}{\partial w_i} = \gamma u_c \mu_i(x). \tag{8}$$

During the neural compensator algorithm implementation, the memory and computational resources of embedded computer is usually limited. For that reason, it is important to reduce the algorithm complexity and the number of weighting coefficients of the BSN to be adapted in each sample time, Fig.4. This type of the neural network is particularly convenient for implementation, since the network has only one-layer of B-spline functions with corresponding weighting coefficients. In each sampling time only two weighting coefficients are adapted, so there is no need for complex mathematical calculations like ones when MLP neural network is used.

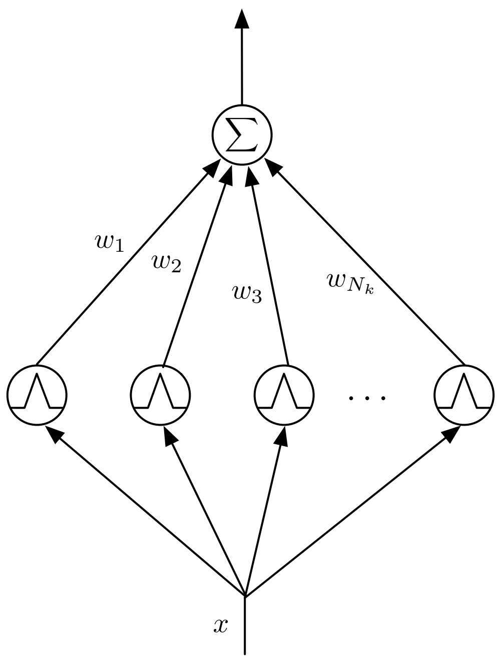

Fig. 4. B-Spline neural network (BSN)

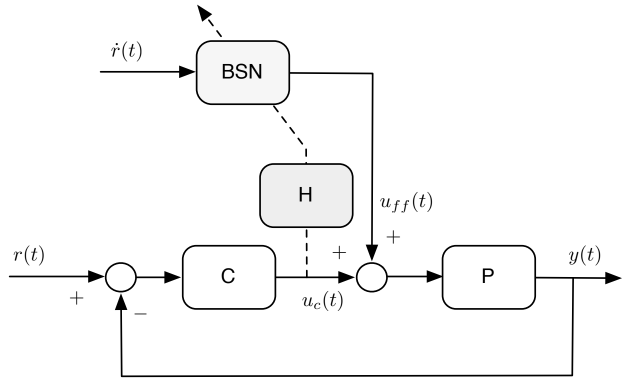

Fig. 5. Block structure of the state feedback controller with BSN compensator

C. Stability of the overall control system

An important issue that often limits implementation of the neural networks in practical applications is how to ensure the stability of the overall control system. This is particularly important when neural network parameters are adapted in an on-line manner. Classical neural network learning algorithms, such as error backpropagation algorithm, cannot guarantee stability due to fact that they consider neural network independently to the rest of the control system (controller and process).

One way to cope with this problem is to use Lyapunov theory to derive stable adaptation law for the neural network parameters. However, the results are very much dependent on the choice of the Lyapunov function. Another approach that originates from Iterated Learning Control (ILC) is based on frequency domain analysis of the overall control system. Since the control scheme used in this paper is essentially Learning Feedforward Control (LFFC) [12], which can be considered as a special case of ILC, the latter approach is adopted in this paper for finding the necessary stability conditions. General stability condition for the LFFC schemes is given by, [12]:

$$|1 - \gamma T(j\omega)| < 1, \tag{9}$$

where $T(j\omega)$ complementary sensitivity function. It is clear that condition (9) may be satisfied for $\omega \in \mathbb{R}^+$ only if $T(\jmath\omega)$ is positive real function. However, in most practical applications this condition is violated for some frequency band, typically for higher frequencies. In order to solve this problem Velthuis et al. [11],[12] used approach based on Fourier analysis of the compensation signal u_{ff} to find minimal width of the B-spline functions d and maximal value of the learning rate γ that guarantee overall control system stability. These values depend on the shape of the negative complementary sensitivity function $-T(j\omega)$ and above all by the frequency where condition (9) ceases to be satisfied. Such the approach, however, often gives relatively large values for d_{min} and consequently significantly limits BSN approximation capability.

In order to overcome this limitation we have augmented the original approach by introducing the addition filter $H(s)$ for BSN network adaptation signal u_C, as shown in Fig. 5:

$$u_C^* = H(s)u_C. \tag{10}$$

General stability condition in that case is slightly different to one given by equation (10):

$$|1 - \gamma H(j\omega)T(j\omega)| < 1 \tag{11}$$

Since the minimum width of the B-spline functions is now determined by the shape of the $-H(j\omega)T(j\omega)$, additional filter $H(j\omega)$ can be considered as loop shaping filter.

Using the procedure proposed in [12] minimal width of B-spline functions that ensures closed loop stability is given by:

$$d_{\min} = \frac{2\pi}{\omega_1}, \tag{12}$$

where ω_1 is the frequency where phase characteristic of $-H(s)T(s)$ is equal to:

$$\varphi_1 = \text{acos}\left(-0.0147\frac{|-H(j\omega)T(j\omega)|_\infty}{\min\limits_{\omega\in\mathbb{R}^+|\cos\varphi<0}(-H(j\omega)T(j\omega))}\right). \tag{13}$$

Once the width of the B-splines d is obtained, learning rate γ should satisfy the following condition:

$$\gamma \leq \frac{4T_s}{|-H(j\omega)T(j\omega)|_\infty d}, \tag{14}$$

where $|\cdot|_\infty$ is infinity norm representing peak value of the $|-H(j\omega)T(j\omega)|$ while T_s is sample time of the compensation algorithm.

It is important to note that stability conditions (12), (13) and (14) are derived for a special case of LFFC, so called time-indexed LFFC, where the input to BSN network is not physical system variable (e.g. position, velocity) but

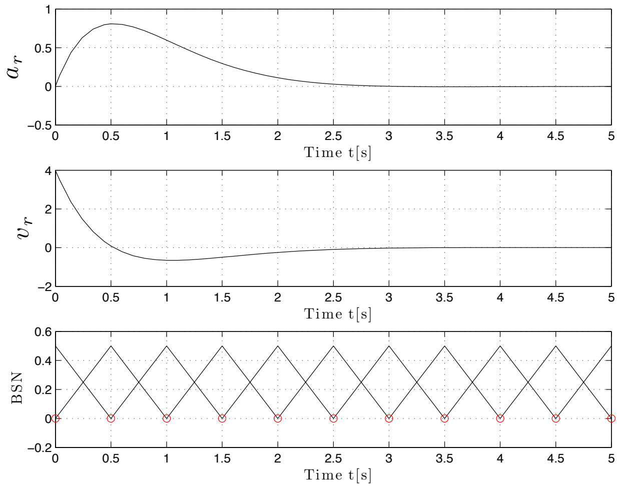

Fig. 6. Reference velocity and acceleration and BSN network output

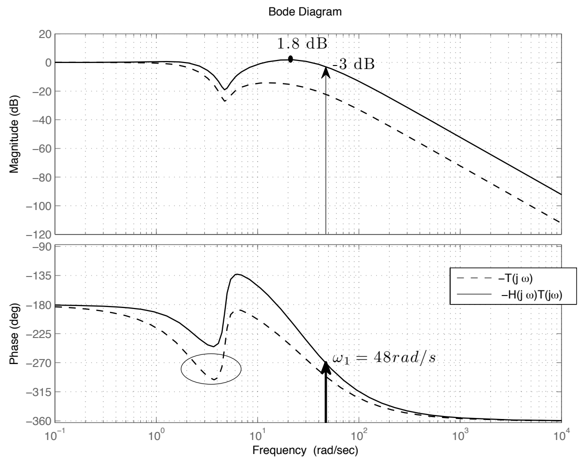

Fig. 7. Bode diagrams of $-T(j\omega)$ and $-H(j\omega)T(j\omega)$

the time t. Such the approach assumes that it is possible to establish unique mapping between the time t and the physical system variables of interest.

Knowing d_{min} for the time-indexed LFFC and reference signal $r(t)$ it is possible to calculate minimal B-splines width for the case when the inputs to BSN are reference and/or its derivatives. This can be easily done by analyzing the worst case, assuming the position reference in a form of filtered step signal. By choosing the 2nd order model reference filter it is possible to exactly calculate reference velocity $v_r(t)$ and acceleration $a_r(t)$, as shown in Fig. 6. It is clear that peak value of the acceleration reference occurs at $t = 0$ (here it is assumed that step reference start at $t = 0$) and this value will define the minimal width of the B-spline functions in term of physical system variable values (velocity in our case). Therefore, minimal width of B-splines functions for velocity driven BSN network can be calculated as follows:

$$d_{\min,v} = \int_0^{d_{\min}} a_r(t)dt = v_r(t)|_0^{d_{\min}} = v_r(d_{\min}). \quad (15)$$

IV. Controller and Friction Compensator Design

Experimental verification of the B-spline neural network based friction compensator has been performed on the experimental crane model, Single Pendulum Gantry (SPG), shown in Fig.1 and described in section II.

The control system structure, used in this paper, with linear state feedback controller (C) and additional friction compensator (BSN) is shown in Fig. 5. Linear feedback controller C is designed for an ideal process, i.e. nonlinear effects and higher order dynamics are neglected. The output of the feedback controller u_C is considered as a control performance measure and thus it is used for BSN on-line learning.

The friction compensator (BSN) is located in the feedforward loop and input signal to the B-spline network is velocity reference, since it is assumed that friction is velocity dependent.

A. Linear Controller Design

Linear state feedback controller (C) is designed using the pole placement approach according to the control requirements, [5]. These requirements are expressed in terms of maximum overshoot σ_m and settling time t_m:

$$\sigma_m = 100e^{\left(-\frac{\xi\pi}{\sqrt{1-\xi^2}}\right)} \leq 5\% \quad (16)$$

$$t_s = \frac{4}{\xi\omega_n} \leq 2.2s \quad (17)$$

Two closed loop poles p_1 and p_2 are dominant and they are chosen to meet control system requirements. Other two poles p_3 and p_4 are chosen arbitrary, in order to have minimal influence on the system behavior. Calculated closed loop poles are

$$\begin{aligned} p_1 &= -1,8182 + 1,9067j \\ p_2 &= -1,8182 - 1,9067j \\ p_3 &= -20 \\ p_4 &= -40 \end{aligned} \quad (18)$$

For linearized model (3) and (4) of the SPG, the following gain vector is obtained

$$K = [160.5347 \ \ -210.625 \ \ 88.0092 \ \ 23,4776] \quad (19)$$

B. Friction Compensator Design

As a first step in compensator design the filter $H(s)$ need to be chosen. In order to achieve smaller minimal B-splines width it is necessary to keep phase diagram of $-H(j\omega)T(j\omega)$ between $-90°$ and $-270°$ in as wide as possible frequency band. Since phase diagram of $-T(j\omega)$ drops below $-270°$ for $2.4 < \omega < 4.5$ (see Fig. 7) it is necessary to compensate it by introducing the phase lead correction:

$$H(s) = \frac{1 + T_1 s}{1 + T_2 s}, \quad (20)$$

with $T_1 = 2\,s$ and $T_2 = 0.2\,s$.

Minimal B-spline width for time-indexed LFFC calculated according (12) and (13) is given by:

$$d_{\min} = 0.13s \quad (21)$$

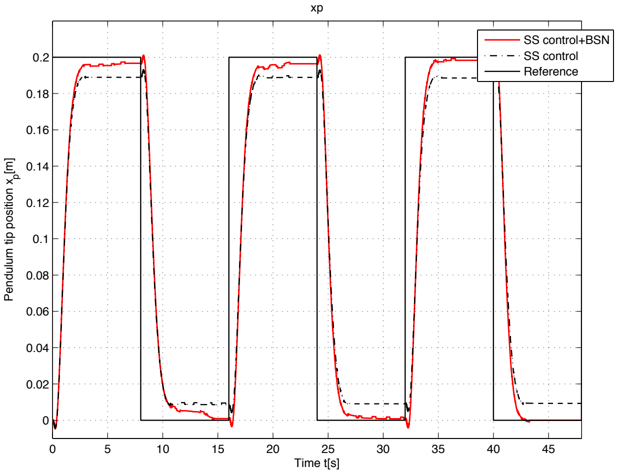

Fig. 8. Position reference and responses of the SPG control systems with and without BSN compensator

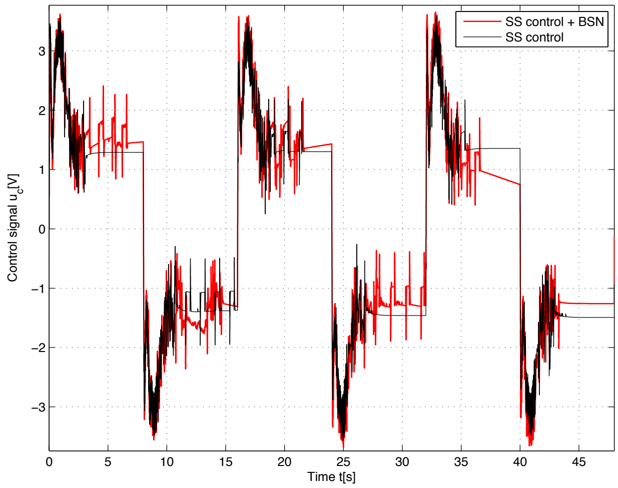

Fig. 9. Control signals of the SPG control systems with and without BSN compensator

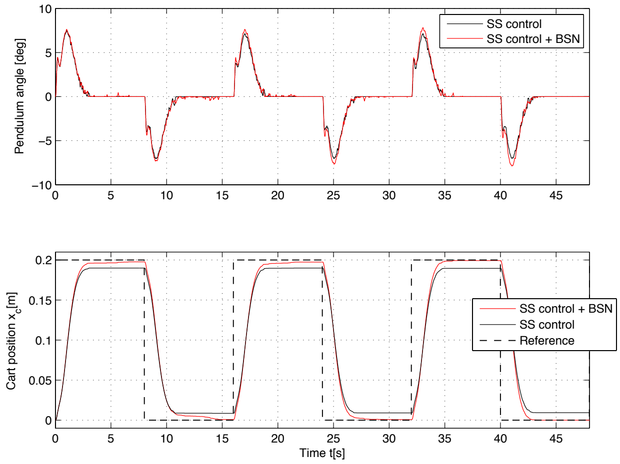

Fig. 10. Pendulum angle and cart position of the SPG control systems with and without BSN compensator

while the maximum learning rate is obtained using equation (14) and assuming sample rate $T_s = 0.001s$:

$$\gamma_{\max} = 0.025. \tag{22}$$

As a reference model 2nd order filter, given by:

$$G_m = \frac{\omega_0^2}{s^2 + 2\zeta\omega_0 s + \omega_0^2}, \tag{23}$$

is used, where $\omega_0 = 2$rad/s and $\zeta = \sqrt{3}/2$. Using the equation (15) minimal B-splines width $d_{\min,v}$ for the velocity driven BSN network is:

$$d_{\min,v} = 0.35[m/s]. \tag{24}$$

As a compensator B-spline neural network with 8 2nd order B-spline functions is used. The width of each particular function is set to $d = 0.35$, while the learning rate is set to $\gamma = 0.02$. It is apparent that such the selection of the BSN parameters ensures the stability of the BSN learning process.

V. Experimental Results

For SPG control, Quanser Q3 ControlPaQ-FW integrated with Matlab 2008b/Simulink Real-time Workshop toolbox is used, together with Quanser UPM 1503/2405 power supply module.

During experimental verification of the compensation algorithm two types of the reference signals were used: (i) step signal filtered through 2$^{\text{nd}}$ order reference model and (ii) sinusoidal signal.

In Fig.8 the reference position and position responses of the control systems with and without B-spline network (BSN) are shown. It can be seen that the position error of the control system with BSN compensator is almost eliminated after a few reference sequences. At the start, initial network coefficients are set to zero (assuming no a-priory knowledge). After that, networks coefficients are updated through the on-line learning mechanism, gradually reducing reference tracking error (Fig. 8).

In Fig 9 the control signals for the cases with and without BSN friction compensator are shown. It is apparent that control system with BSN compensator produces more active control signal in steady state, i.e. when cart velocity is relatively low and static friction become dominant. However, after three periods of the reference signal control signal become steady which indicates that BSN network has learned the friction characteristic.

Finally, in Fig.11 sinusoidal position reference tracking for the control systems with and without BSN compensator are shown. Without BSN compensator substantial tracking error occurs near peak values of the reference signal, i.e. at low velocities. This error is significantly reduced by adding the friction compensator. However, almost constant tracking error still remained but this error is not related to the friction effect but to the limitation of the designed feedback controller.

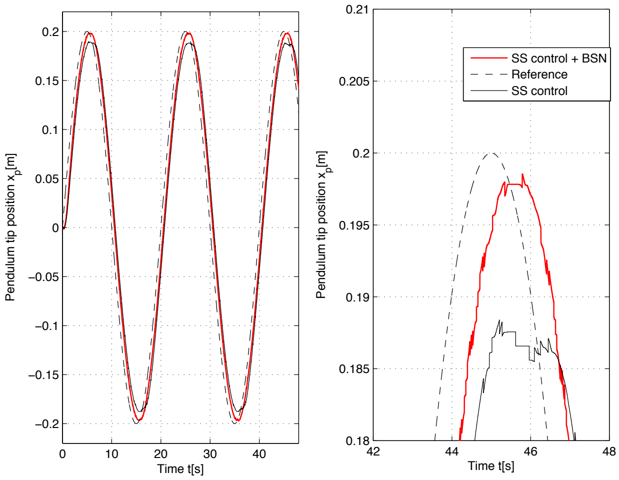

Fig. 11. Responses of SPG control systems with and without BSN compensator to sinus reference signal

VI. Conclusion

The effectiveness of the B-spline self-learning network compensator applied to the gantry crane system for the friction compensation has been proven. The experiments made on Single Pendulum Gantry model, show that position error with friction compensator is practically eliminated. Additionally, loop shaping filter added in BSN network learning loop relaxes the stability constraints on the minimal B-splines width and the maximal learning rate. Finally, it is important to notice that no a-priori information about the friction are needed since neural network parameters are updated in on-line manner.

References

[1] G. Bartolini, N. Orani, A. Pisano, and E. Usai. Load swing damping in overhead cranes by sliding mode technique. In *Decision and Control, 2000. Proceedings of the 39th IEEE Conference on*, volume 2, 2000.

[2] M. Brown and CJ Harris. *Neurofuzzy adaptive modelling and control*. Prentice Hall, 1994.

[3] G. Corriga, A. Giua, and G. Usai. An implicit gain-scheduling controller for cranes. *IEEE Transactions on Control Systems Technology*, 6(1):15–20, 1998.

[4] Q.I. Educate. IP01 and IP02 Single Inverted Pendulum User Manual. *MultiQ User Manual, MultiQ User Manual*, 2003.

[5] S. Haykin. *Neural networks: a comprehensive foundation*. Prentice Hall PTR Upper Saddle River, NJ, USA, 1994.

[6] P. Korondi. Tensor product model Transformation-based Sliding Surface Design. *Acta Polytechnica Hungarica*, 3(4), 2006.

[7] Z. Kovačić and S. Bogdan. *Fuzzy controller design: theory and applications*. CRC Press, 2006.

[8] IJ Nagrath. *Control systems engineering*. New Age International, 2005.

[9] Gerco Otten, Theo J. A. De Vries, Adrian M. Rankers, and Erik W. Gaal. Linear motor motion control using a learning feedforward controller. *IEEE/ASME Transactions on Mechatronics*, 2:179–187, 1997.

[10] T. Popadić, F. Kolonić, and A. Poljugan. A Fuzzy Control Scheme for the Gantry Crane Position and Load Swing Control. In *S MIPRO-m u društvo znanja. 29ˆ th International Convention MIPRO 2006. CTS&CIS, Computers in Technical Systems, Intelligent Systems and Microelectronics*, 2006.

[11] Wubbe J. R. Velthuis, Theo J. A. de Vries, Pieter Schaak, and Erik W. Gaal. Stability analysis of learning feed-forward control. *Automatica*, 36(12):1889 – 1895, 2000.

[12] Wubbe J. R. Velthuis, Theo J. A. de Vries, Pieter Schaak, and Erik W. Gaal. Stability analysis of learning feed-forward control. *Automatica*, 36(12):1889 – 1895, 2000.

[13] Z. Wang and B. Surgenor. Performance Evaluation on the Optimal Control of a Gantry Crane. In *7th Biennial ASME Conference Engineering System Design and Analysis, Manchester, UK*, 2004.